PNAS RESEARCH ARTICLE | ENVIRONMENTAL SCIENCES SUSTAINABILITY SCIENCE OPEN ACCESS

Mitigation and adaptation emissions embedded in the broader climate transition

Corey Lesk[a,b,1,2], Denes Csala[c,d,e], Robin Hasse[f], Sgouris Sgouridis[g], Antoine Levesque[f], Katharine J. Mach[h,i], Daniel Horen Greenford[j], H. Damon Matthews[j], and Radley M. Horton[a]

Edited by William Clark, Harvard University, Cambridge, MA; received December 30, 2021; accepted October 4, 2022

Climate change necessitates a global effort to reduce greenhouse gas emissions while adapting to increased climate risks. This broader climate transition will involve large-scale global interventions including renewable energy deployment, coastal protection and retreat, and enhanced space cooling, all of which will result in CO_2 emissions from energy and materials use. Yet, the magnitude of the emissions embedded in these interventions remains unconstrained, opening the potential for underaccounting of emissions and conflicts or synergies between mitigation and adaptation goals. Here, we use a suite of models to estimate the CO_2 emissions embedded in the broader climate transition. For a gradual decarbonization pathway limiting warming to 2 °C, selected adaptation-related interventions will emit ∼1.3 $GtCO_2$ through 2100, while emissions from energy used to deploy renewable capacity are much larger at ∼95 $GtCO_2$. Together, these emissions are equivalent to over 2 y of current global emissions and 8.3% of the remaining carbon budget for 2 °C. Total embedded transition emissions are reduced by ∼80% to 21.2 $GtCO_2$ under a rapid pathway limiting warming to 1.5 °C. However, they roughly double to 185 $GtCO_2$ under a delayed pathway consistent with current policies (2.7 °C warming by 2100), mainly because a slower transition relies more on fossil fuel energy. Our results provide a holistic assessment of carbon emissions from the transition itself and suggest that these emissions can be minimized through more ambitious energy decarbonization. We argue that the emissions from mitigation, but likely much less so from adaptation, are of sufficient magnitude to merit greater consideration in climate science and policy.

climate change | mitigation | adaptation | embedded emissions

Significance

Adapting to increasing climate risks while deploying renewables to stabilize the climate will require large amounts of energy and materials, which will initially cause emissions. We provide an estimate of the CO_2 emissions embedded in this broader climate transition, which were previously poorly quantified. Fossil fuel energy use to deploy renewables contributes the vast majority of embedded emissions, with a much smaller contribution from adaptation. As a result, embedded emissions increase substantially for slower decarbonization pathways. However, when renewables are rapidly deployed, the ongoing transition can be powered by cleaner energy, minimizing embedded emissions. Our results demonstrate an underappreciated benefit of enhanced climate ambition and the importance of accounting for embedded transition emissions to achieve climate objectives.

The diverse dangers of human-induced climate change demand two major international efforts: reducing greenhouse gas (GHG) emissions enough to keep warming below a specified limit (1–4), and adapting infrastructure and other human activities to support societal goals at that level of warming (5–9). The twin global projects of climate mitigation and adaptation can be characterized as two components of a broader climate transition, in which temperatures stabilize and societies adapt to the impacts. Such a transition will involve a significant investment of economic activity and energy use, which will generate CO_2 emissions as long as they are powered by fossil fuel combustion.

Among a wide array of potential mitigation and adaptation interventions, we investigate three illustrative examples. We select examples that are particularly widely required, energy intensive, and likely to be deployed (*Materials and Methods*), and thus together provide a reasonable bounding of the likely emissions from the full basket of interventions comprising the broader climate transition. First, mitigating CO_2 emissions from the energy sector necessitates the mass construction of renewable electricity generating capacity, which we term deploying renewables. Second, climate warming due to historical and future emissions will make space cooling necessary in new regions and increase the duration and intensity of its use globally (5, 10). We term this additional space cooling attributable to warming as adaptive space cooling. Third, sea-level rise (SLR) caused by historical and future emissions will require the construction of coastal flood defenses and relocation of coastal settlements across a potentially vast portion of the global coastline, which we collectively term coastal adaptation (6, 8, 11). Each of these interventions will require energy to build and operate, which we call its embedded energy. Because renewable capacity is presently insufficient, this embedded energy must be initially powered by fossil fuels (12), resulting in embedded CO_2 emissions.

Refining estimates of remaining carbon budgets as a measure of the emissions "runway" for the transition to a stable climate has been a topic of great importance to climate science and policy (13). Embedded emissions from mitigation and adaptation effectively reduce the space available for remaining CO_2 emissions in other economic

Author contributions: C.L., D.C., R.H., S.S., A.L., K.J.M., D.H.G., H.D.M., and R.M.H. designed research; C.L., D.C., and R.H. performed research; D.C. and R.H. contributed new reagents/analytic tools; C.L., D.C., and R.H. analyzed data; and C.L., D.C., R.H., S.S., A.L., K.J.M., D.H.G., H.D.M., and R.M.H. wrote the paper.

The authors declare no competing interest.

This article is a PNAS Direct Submission.

[1]To whom correspondence may be addressed. Email: Corey.S.Lesk@dartmouth.edu.

[2]Present address: Department of Geography, Neukom Institute, Dartmouth College, Hanover, NH 03755.

This article contains supporting information online at http://www.pnas.org/lookup/suppl/doi:10.1073/pnas.2123486119/-/DCSupplemental.

Published November 21, 2022.

Table 1. Three decarbonization pathways explored in this study, with equivalent IPCC terminology and mean warming levels

Transition intervention	Deploying renewables	Adaptive space cooling	Coastal adaptation
Quantity of measure	Net sustainable energy transition model (NETSET) + carbon budget	Energy demand generator (EDGE) + warming projections	Coastal impacts and adaptation model (CIAM) + SLR projections
Embedded energy	Simulated in NETSET	Simulated in EDGE	Life cycle analysis (LCA)
Embedded emissions	Emissions factors from LCA + energy mix from NETSET		

sectors. Much effort has been devoted to understanding the economic costs of mitigation (14, 15) and adaptation (6, 11) needed to achieve the broader climate transition. The likely carbon emissions cost of the transition itself, by contrast, has received less attention (16, 17).

Energy use for building the clean energy transition has been suggested as a potentially large source of emissions (12, 18–20), but a holistic global estimate of the aggregate magnitude of these emissions is presently lacking. Further, while energy demand for projected future space cooling has been studied in some regions (5), likely emissions from this and other projected adaptations to climate change (such as coastal adaptation) remain poorly understood. Thus, the potential for embedded emissions from mitigation and adaptation to effectively shorten the emissions runway, or necessitate shifts in economic priorities and investments to respect carbon budgets, remains largely unconstrained.

In this study, we provide an estimate of embedded CO_2 emissions likely to result from mitigation and adaptation across the broader climate transition for the years 2020 to 2100. The wider purpose of this estimate is to assess whether the magnitude of these emissions is relevant from a climate science and policy perspective. We first quantify the emissions embedded in the transition under a gradual 2 °C-consistent future energy and climate pathway (decarbonization pathway).We then reassess these embedded emissions under rapid (1.5 °C consistent) and delayed (2.7 °C consistent) decarbonization pathways to assess their sensitivity to climate ambition (Table 1). To contextualize the scale of the embedded emissions under the three scenarios for climate science and policy, we compare them to remaining carbon budgets in two ways. First, we express total embedded emissions as a percent of the remaining carbon budget within each scenario, examining their magnitude relative to differing decarbonization pathways and warming levels. Second, we compute the emissions under each scenario as a percent of the 1.5 °C remaining carbon budget, assessing their relevance to ideal maximum warming targets under the Paris Agreement (2). We finally identify and discuss key uncertainties and leverage points for addressing potentially important emissions from mitigation and adaptation.

We bring together three existing and widely used sectoral models suited to the goals of this study (Table 2 and *SI Appendix*, Fig. S5). For the simulated decarbonization pathways, we use the net sustainable energy transition (NETSET) model, which simulates total primary energy demand across 12 energy sources (including fossil fuels, nuclear, and renewables) (12). NETSET explicitly simulates embedded energy in deploying energy capacity (i.e., energy investment into building power plants), separately from net energy available to society, based on energy system dynamics constrained by carbon budgets derived from the Intergovernmental Panel on Climate Change (IPCC) Sixth Assessment Report (21). For adaptive space cooling, we use the energy demand generator (EDGE) model (10), which simulates building energy dynamics based on technological and socioeconomic projections. For coastal adaptation, we use the coastal impacts and adaptation model (CIAM) (6), which simulates cost-optimal coastal protection (sea wall length and height) and retreat (population) by combining high-resolution SLR projections with geophysical data and economic assumptions. To develop our estimates, we run these models under a consistent set of carbon budgets, climate model projections based on representative concentration pathway (RCP) emissions scenarios, and socioeconomic inputs for each decarbonization pathway (Table 1). We finally use factors from life cycle analysis (LCA) literature to express model outputs in terms of the quantity of each transition intervention, its embedded energy demand, and the associated embedded CO_2 emissions ensuing from energy and materials use (Table 2).

Results

Table 2 illustrates a roadmap of our results and summarizes the associated methods. First, we present results for the simulated 2 °C gradual decarbonization pathway. We begin by describing the simulated quantities of each intervention (deploying renewables, adaptive space cooling, and coastal adaptation) through 2100, and the underlying drivers of these changes (Fig. 1). We then report the embedded energy requirements to fulfill the increasing quantities of each intervention through the transition (Fig. 2), followed by the associated CO_2 emissions estimates (Fig. 3). Finally, we present key results for the rapid (1.5 °C) and delayed (2.7 °C) decarbonization pathways (Table 1), highlighting the sensitivity of emissions to the transition (Figs. 4 and 5).

Table 2. Rubric of estimates reported and summary of underlying methods

Decarbonization pathway	IPCC equivalent	IPCC description	Remaining carbon budget (GtCO2)*	Mean warming in 2100	Figure
Gradual	RCP2.6	Sustainable development scenario	1,150	2.0 °C	Figs. 1–3
Rapid	RCP1.9	Ambitious scenario to meet Paris Agreement	400	1.5 °C	Figs. 4 and 5
Delayed	RCP4.5	Intermediate scenario	2,150	2.7 °C	Figs. 4 and 5

*Data from table 5.8 in ref. 21.

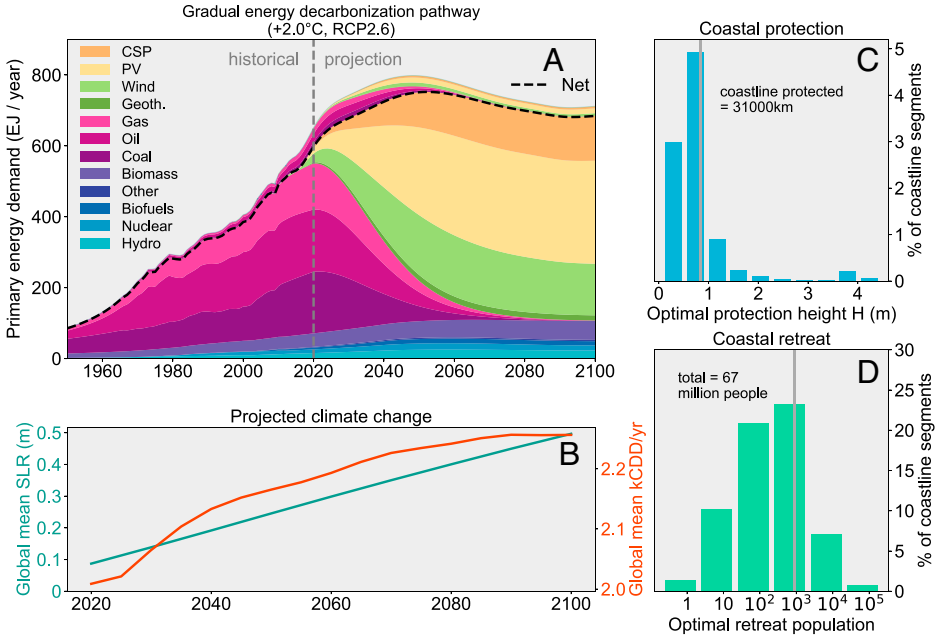

Fig. 1. Simulated quantities of renewable deployment and adaptation under the gradual decarbonization pathway. (*A*) Gradual 2°C decarbonization pathway projected using the NETSET global energy model (respecting a remaining carbon budget of 1,150 $GtCO_2$ and minimum net energy per capita of 2,000 W) (table 5.8 in ref. 21. Colored areas depict time evolution of primary energy demand across energy sources. The dashed black line separates energy investment into building and maintaining energy capacity (*Above*) from net energy available to society (*Below*). The dashed vertical gray line separates historical from projected data. (*B*) Projected climate change forced by GHG emissions under IPCC RCP2.6 sustainable development emissions scenario, which results in an increase in population-weighted global mean CDDs (orange curve) and global mean SLR (blue curve). (*C*) Distribution of cost-optimal coastal protection heights (by coastline segment) over the 2050 to 2100 planning period, projected using the CIAM model. The total coastline protected is the sum of the lengths of protected coastline segments. The vertical gray line shows the global median value. (*D*) Same as *C*, but for cost-optimal retreat population. Note that retreat population is presented on a logarithmic axis.

Quantity of Renewable Energy Deployment and Adaptation in Gradual Decarbonization Pathway. Under the gradual decarbonization pathway projected using NETSET, wind and solar capacity is deployed beginning in 2020 with installation rates averaging 4.5 TW of peak generating capacity per year (TWp/y) over 2020 to 2050 (Fig. 1*A*). Peak capacity signifies the total generating capacity needed to meet maximum power demand. Solar and wind capacity plateaus at ∼100 TWp by 2050, satisfying ∼80% of global primary energy demand (Fig. 1*A*). This deployment of solar and wind—along with smaller increasing contributions from geothermal and scale-limited renewables—drives the near-total displacement of fossil fuels from the energy mix by about 2080.

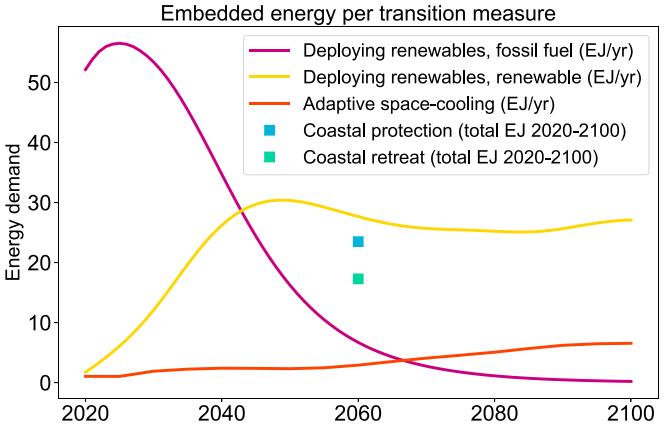

Fig. 2. Embedded energy demand from deploying renewables and adaptation under the gradual decarbonization pathway over 2020 to 2100. The purple curve shows fossil fuel energy embedded in deploying renewables, whereas the yellow curve shows renewable embedded energy (i.e., renewable energy reinvested into deploying renewables). The orange curve shows embedded energy for adaptive space cooling. Energy embedded in coastal protection (blue square) and retreat (green square) are presented as totals over 2020 to 2100, assumed to occur at the midpoint of the transition in 2060.

Continued GHG emissions over the next several decades induce climate warming (Fig. 1*B*). Projected future cooling degree days (CDDs, a measure of cumulative warm weather resulting in space cooling service demand) continue to rise with global climate warming through the 2060s and then plateau through 2100, peaking at around 13% above 2020 levels (Fig. 1*B*, orange line).

By contrast, projected SLR proceeds steadily reaching a global mean of 50 cm by 2100 compared to 2000 (Fig. 1*B*, blue line), reflective of the slower and higher-inertia response of oceans and cryosphere to warming. As a result, we project expanding coastal adaptation in coming decades (Fig. 1 *C* and *D*). We estimate that over the 2050 to 2100 planning period, protective infrastructure will be cost optimal over 31,000 km of coastline or around 3% of the global coastline, protecting 130 million people (Fig. 1*C* and *SI Appendix*, Fig. S1*A*). The median optimal protection height is around 1 m, excluding wave run-up and initial underprotection. Additionally, some degree of coastal retreat would be cost optimal across a much larger ∼70% of coastal segments, representing 67 million people globally (Fig. 1*D* and *SI Appendix*, Fig. S1*B*). These projections are comparable to other recent estimates (8) and are determined largely by CIAM's consideration of future geophysical exposure, land value and capital density, and adaptation and flood damage costs. CIAM does not directly simulate political feasibility of the cost-optimal adaptation. Coastline segments where neither retreat nor protection are optimal are concentrated in sparsely populated desert and high latitude areas (*SI Appendix*, Fig. S1). Protected segments tend to be more densely populated (by a median factor of 5) and have higher climatological 1-in-1-y storm surges (by ∼25%) than segments where retreat is optimal (*SI Appendix*, Fig. S1 *C–F*).

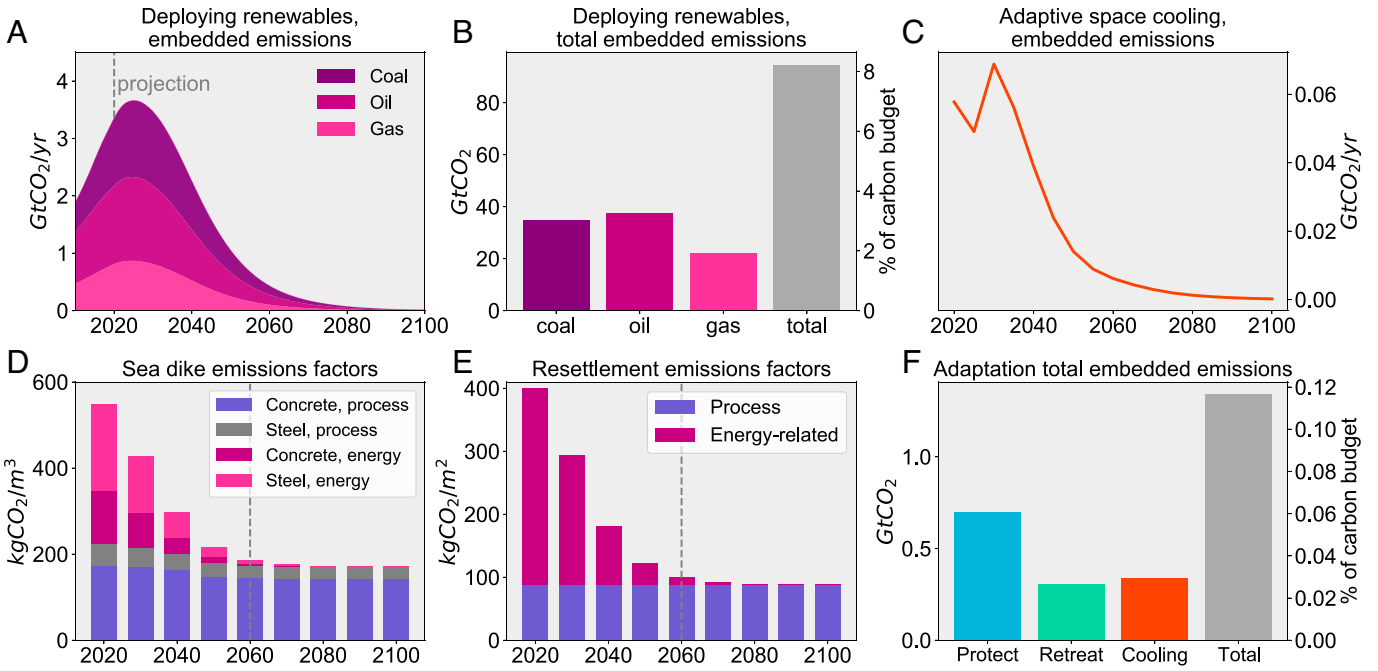

Fig. 3. Embedded mitigation and adaptation CO_2 emissions under the gradual decarbonization pathway. (*A*) Time evolution of embedded emissions from deploying renewables as projected in NETSET under gradual decarbonization. Dashed vertical line separates historical from projected data. (*B*) Total embedded emissions in deploying renewables over 2020 to 2100 in absolute units and as a percent of the remaining carbon budget for 2 °C. (*C*) Time evolution of adaptive cooling embedded emissions based on energy demand from EDGE and energy mix from NETSET. (*D*) Estimated emissions factors over time by source for materials in modeled sea dike. (*E*) Estimated emissions factors over time by source for resettlement housing. Data in *D* and *E* are based on LCA literature, decarbonization of the energy mix as projected in NETSET, and decarbonization of steel and cement process emissions based on IEA scenarios. Vertical dashed line denotes the midpoint of the transition, at which coastal adaptations are assumed to take place. (*F*) Total embedded emissions from coastal protection, coastal retreat, and adaptive cooling over 2020 to 2100, in absolute units and as a percent of the remaining carbon budget for 2 °C. Remaining carbon budgets are from table 5.8 in ref. 21.

Energy Embedded in Transition under Gradual Decarbonization Pathway. Deploying renewables results in energy demands throughout the 21st century, at first primarily satisfied by fossil fuels (Fig. 2, purple curve), then increasingly by renewables themselves (i.e., reinvestment of renewable energy into deploying further renewable capacity, Fig. 2, yellow curve). The primary energy embedded in deploying renewables totals 930 PWh (3,350 EJ) over 2020 to 2100, of which 405 PWh (1,460 EJ) or 43% are provided by fossil fuels (Fig. 2). To put these numbers in perspective, the world consumed 155 PWh (560 EJ) of primary energy in 2020. Our global estimates are consistent with a comparable national study for Denmark (22).

Projected adaptations contribute additional, though much smaller, energy requirements over coming decades. As a result of projected higher CDDs, additional energy demand for climate-adaptive space cooling is projected by EDGE to rise gradually throughout the century to around 5 EJ/y by 2100 compared to the current climate (Fig. 2, orange curve). We estimate that energy embedded in coastal adaptations amounts to around 20 EJ for retreat and 25 EJ for protection in aggregate over 2020 to 2100, which we present as occurring at the midpoint of the transition in 2060 (Fig. 2, squares, see *Materials and Methods*).

Emissions Embedded in Transition under Gradual Decarbonization Pathway. The CO_2 emissions resulting from energy embedded in deploying renewables and adaptation depend on the emissions intensity of energy, which we derive from the US Energy Information Administration global energy statistics in the 2019 International Energy Outlook. We estimate the average emissions intensity of major fossil fuels to be around 90 tCO_2/TJ for coal, 60 tCO_2/TJ for oil, and 50 tCO_2/TJ for natural gas (*SI Appendix*, Table S1).

Based on these emissions factors and the evolution of the simulated energy mix through the transition (Fig. 1*A*), we project that the emissions embedded in deploying renewables peak in 2025 at 3.8 $GtCO_2$/y before steeply declining (Fig. 3*A*). The decline is due to the replacement of fossil fuels by renewable energy in the overall energy mix, resulting in a lower emissions intensity of primary energy used to deploy further renewable capacity (*SI Appendix*, Fig. S2*B*). In total over 2020 to 2100, coal contributes 35 $GtCO_2$, oil around 37 $GtCO_2$, and gas around 23 $GtCO_2$ for a total embedded emissions of ~95 $GtCO_2$, equivalent to 2.5 y of current global emissions and over 8% of the remaining carbon budget for 2 °C (Fig. 3*B*). These emissions estimates for deploying renewables are robust to varying two key energy system change assumptions in the NETSET model. Compared to our default assumptions, total emissions differ by ±5% on average (−7.5% minimum, 20.7% maximum) across eight sets of alternative assumptions of future net energy demand per capita and fossil fuel phase out start year (*SI Appendix*, Fig. S3).

Embedded emissions from adaptive space cooling follow a similar evolution to those from deploying renewables. They peak around 2030 at ~70 $MtCO_2$/y (about 2% of the peak embedded emissions from deploying renewables), before declining steeply beginning in the 2040s (Fig. 3*C*). This decline occurs even as primary energy demand from cooling rises (Fig. 2), compensated by reductions in the emissions intensity of energy as renewables displace fossil fuels in the energy mix (Fig. 1*A*).

For coastal adaptation, we separately simulate energy-related versus process emissions in the production of materials like steel and cement. Energy-related emissions arise from fossil fuel combustion to produce the heat needed to manufacture steel and cement. We simulate mitigation of these emissions via the substitution of fossil fuels for renewables under the decarbonization

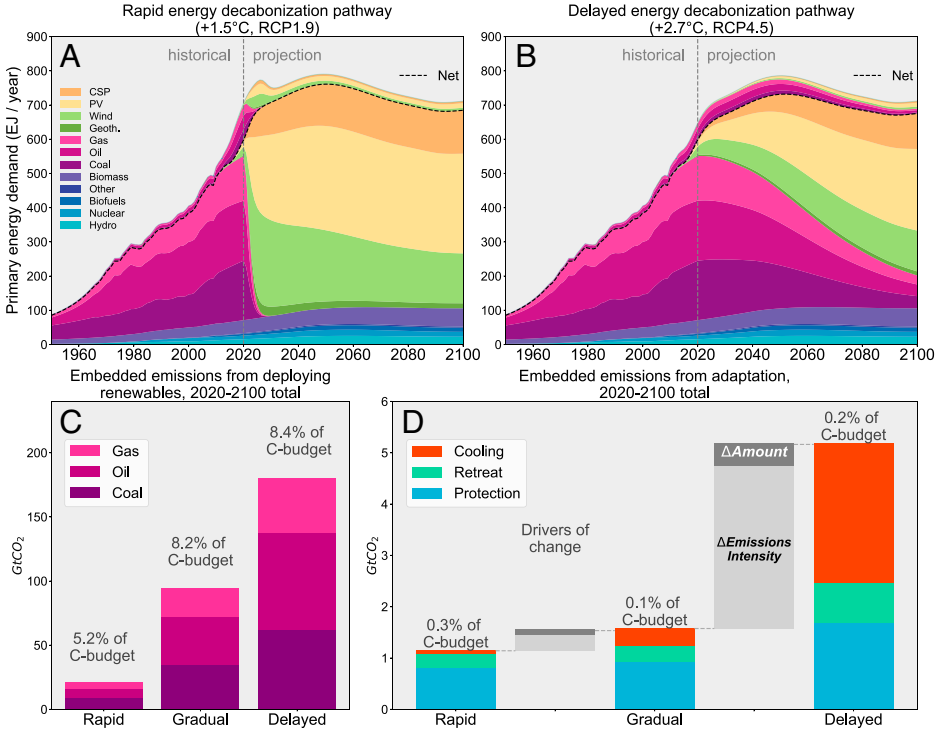

Fig. 4. Comparative mitigation and adaptation CO_2 emissions from a rapid, gradual, and delayed transition. (*A*) Rapid decarbonization pathway limiting warming to 1.5 °C (same as Fig. 1*A*, except respecting a smaller carbon budget of 400 $GtCO_2$). Colored areas depict time evolution of primary energy demand across energy sources. The dashed black line separates energy investment into energy (*Above*) from net energy available to society (*Below*). The dashed gray line separates historical from projected data. (*B*) Same as *A* but for the delayed decarbonization pathway with warming ~2.7 °C in 2100 (respecting a larger carbon budget of 2,150 $GtCO_2$). Remaining carbon budget estimates are from table 5.8 in ref. 21. (*C*) Total embedded emissions from deploying renewables over 2020 to 2100 for the three decarbonization pathways. Annotations show emissions as percentages of respective carbon budgets. (*D*) Total embedded emissions from coastal retreat, coastal protection, and adaptive cooling over 2020 to 2100 for the three decarbonization pathways. Gray floating bars show drivers of change in total adaptation embedded emissions between the three cases, partitioned (as an average across the three adaptations) into a component due to change in amount of adaptation versus change in emissions intensity of primary energy.

pathway. By contrast, process emissions arise from chemical reactions currently used to transform raw materials into cement and steel, and they must be separately mitigated by using alternative chemical reactions. We simulate mitigation of process emissions via low-carbon production process scenarios derived from the

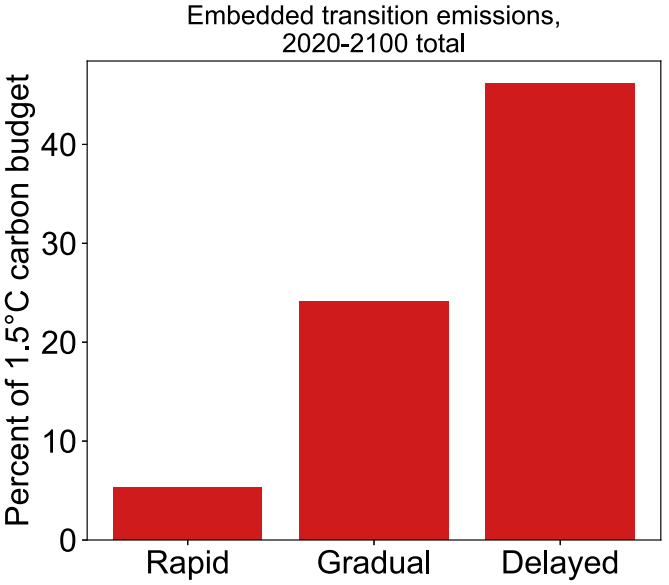

Fig. 5. Total embedded emissions in the transition relative to the 1.5 °C remaining carbon budget. Total embedded emissions from deploying renewables and selected adaptations over 2020 to 2100 for the three decarbonization pathways expressed as a percent of the 1.5 °C remaining carbon budget (400 $GtCO_2$, table 5.8 in ref. 21).

International Energy Agency Technology Roadmaps (23, 24) (*Materials and Methods*). Estimated emissions intensities from energy use decline rapidly with increasing renewable capacity (Fig. 3 *D* and *E*, purple bars), while process emissions from the production of steel and cement decline gradually with technological improvement (Fig. 3 *D* and *E*, blue and gray bars). Energy-related emissions dominate process emissions at the start of the transition (by a factor of 1.5 for dikes and 4 for resettlement), but contribute <10% of emissions by the assumed time of adaptation in 2060 (Fig. 3 *D* and *E*). In other words, by the time coastal adaptation occurs in our model, it is reliant on a cleaner energy mix and occurs with a 50 to 75% lower emissions intensity than at present.

In aggregate over 2020 to 2100, coastal protection contributes ~0.7 $GtCO_2$ of embedded emissions, while coastal retreat and adaptive cooling each contribute around 0.3 $GtCO_2$ (Fig. 3*F*). Total adaptation emissions through 2100 are thus much smaller than emissions from fossil fuel energy investment into renewable capacity, amounting to ~1.3 $GtCO_2$ or around 0.1% of the remaining carbon budget, with a dominant share arising from coastal protection.

Sensitivity of Emissions Embedded in Deploying Renewables to Decarbonization Pace. The future pace of decarbonization is highly uncertain: Nations have agreed to rapidly mitigate emissions and limit warming to ideally 1.5 °C, but current global climate policies are insufficient to meet this goal and are likely to lead to ~2.7 °C of warming by 2100 (25). To understand the implications of decarbonization pathway uncertainty for emissions embedded in the broader climate transition, we

examine two alternative decarbonization pathways: a rapid one limiting warming to 1.5 °C, and a delayed one consistent with current policies leading to 2.7 °C warming.

Under the rapid decarbonization pathway, the renewable capacity installation rate averages 5.9 TWp/y over 2020 to 2050, 30% greater than the rate for the gradual pathway and peaks strongly in the 2020s at over 10 TWp/y (Fig. 4*A*). We consider this pathway more illustrative than realistic, since these mean and peak renewable capacity installation rates are unlikely to be techno-politically feasible (26). Fossil fuels are virtually eliminated from the energy mix by 2030, and renewable deployment is subsequently powered by reinvestment of renewable energy (*SI Appendix*, Fig. S2*B*). Earlier deployment of renewables decreases the emissions embedded in renewable deployment to 20 $GtCO_2$ (Fig. 4*C*).

By contrast, a cumulative 180 $GtCO_2$ of emissions are embedded in deploying renewables under delayed decarbonization (Fig. 4*B*), nearly double those from the gradual pathway and nine times greater than the rapid pathway (Fig. 4*C*). The mean installation rate of renewable capacity (2.6 TWp/y over 2020 to 2050) is roughly halved compared to the rapid transition (*SI Appendix*, Fig. S2*A*). This leads to a higher share of fossil fuels in the energy mix throughout the 21st century (e.g., 47% in 2050, compared to 15% under gradual and <1% under rapid, Fig. 4*C*). Consequently, a majority of the energy embedded in deploying renewables is derived from fossil fuels (73% in total over 2020 to 2100, compared to 43% under gradual and 11% under rapid decarbonization, *SI Appendix*, Fig. S2*B*).

Sensitivity of Emissions Embedded in Adaptation to Decarbonization Pace. Avoided emissions under rapid decarbonization limit climate change and projected adaptation. Sea levels rise by 14% less than under gradual decarbonization (43 cm by 2100, *SI Appendix*, Fig. S2*C*), resulting in a 10% decrease in coastal protection (although retreat population rises by 4%). Under the delayed decarbonization pathway, greater total emissions accelerate global mean SLR (60 cm by 2100, or 20% more than the gradual transition, *SI Appendix*, Fig. S2*C*), resulting in 13% more coastal protection and an 11% larger retreat population than under rapid decarbonization. Projected CDDs are boosted by 8% under delayed decarbonization and reduced by 4% under rapid decarbonization, compared to the gradual transition by 2100 (*SI Appendix*, Fig. S2*C*).

Although they contribute only a small fraction of total emissions embedded in the transition, adaptation emissions increase nonlinearly with cumulative emissions across the pathways. Total adaptation emissions are reduced by ∼10% to ∼1.2 $GtCO_2$ under rapid decarbonization compared to the gradual pathway, but triple under the delayed pathway for a total of ∼5 $GtCO_2$ over 2020 to 2100 (Fig. 4*D*). Reductions in embedded emissions with rapid decarbonization are dominated by an 80% reduction in cooling emissions. Conversely, embedded emissions from all adaptations expand substantially in the delayed pathway, increasing by 80% for coastal protection (from ∼1 to ∼1.8 $GtCO_2$), by a factor of 2.7 for coastal retreat (∼0.3 to ∼0.8 $GtCO_2$), and by a factor of 8 for adaptive cooling (∼0.3 to ∼2.4 $GtCO_2$).

These increases in emissions embedded in adaptation are driven primarily (∼90%) by an increased global emissions intensity of energy as the decarbonization pace slows (light gray bars in Fig. 4*D*), with a secondary contribution of ∼10% from a higher amount of adaptation (i.e., higher energy demand, dark gray bars in Fig. 4*D*). Increased emissions from cooling are additionally raised by lower primary-to-final conversion efficiency of fossil fuels compared to renewables, boosting primary energy demand by 30% under delayed compared to rapid decarbonization (*SI Appendix*, Fig. S2*C*). Thus, fractional changes in adaptation emissions resulting from slower transitions far exceed the fractional change in adaptation amounts driven by geophysical climate impacts, because the resulting adaptation energy demand is met by far "dirtier" energy.

Increased energy demand and emissions from adaptive space cooling will likely be offset to some extent by reduced space heating with warming (*SI Appendix*, Fig. S4). Because of modeling limitations, we isolate our explicit energy and emissions projections for heating from our main analysis, but briefly present results here. Under simple schematic projection scenarios (*Materials and Methods*), total avoided heating emissions over 2020 to 2100 amount to 0.15 $GtCO_2$ for rapid decarbonization, outweighing enhanced emissions from space cooling by a factor of three (*SI Appendix*, Fig. S4*G*). However, emissions avoided from decreased heating (0.3 $GtCO_2$) are equal in magnitude to embedded emissions for cooling under gradual decarbonization (*SI Appendix*, Fig. S4*H*). With delayed decarbonization, avoided emissions from decreased heating (1.0 $GtCO_2$) amount to only half the embedded emissions for cooling (*SI Appendix*, Fig. S4*I*).

Sensitivity of Total Emissions Embedded in Transition to Decarbonization Pace. Compared to the gradual decarbonization pathway, total emissions embedded in the transition (deploying renewables + adaptation) decrease by 80% under the rapid pathway (21.2 $GtCO_2$), and roughly double under the delayed pathway (185 $GtCO_2$). In other words, total embedded emissions differ by a factor of ∼9 between the rapid and delayed pathways. Although emissions embedded in adaptation increase strongly across the pathways, the sensitivity of total embedded emissions is driven by deploying renewables, which contributes the large majority of total emissions embedded in the transition.

To assess the climate science and policy relevance of emissions embedded in the transition across the pathways, we compare them to remaining carbon budgets in two ways. Total emissions embedded in the transition as a percent of each pathway's respective remaining carbon budget is relatively static (5.5% for rapid, 8.3% for gradual, and 8.6% for delayed decarbonization, sum of estimates in Fig. 4 *C* and *D*), despite large absolute increases in total emissions embedded in the transition across the decarbonization pathways. This comparison contextualizes the embedded emissions relative to the different warming levels assumed by each pathway.

However, the opposite is true when the emissions for each pathway are expressed as a percent of the 1.5 °C remaining carbon budget. The 2.0 and 2.7 °C of warming attained under the gradual and delayed pathways would likely have severe impacts on humans and ecosystems. Thus, the 1.5 °C remaining carbon budget is also a meaningful denominator of relevance to climate science and policy, being the ideal maximum warming target set in the Paris Agreement to avoid dangerous impacts (2). Embedded transition emissions reach 24% of the 1.5 °C carbon budget under the gradual pathway and 46% under the delayed (Fig. 5). In other words, the emissions embedded in the broader climate transition under the delayed pathway, which is most aligned with current global policies, amount to nearly half of the 1.5 °C target.

Discussion

Under the gradual decarbonization pathway, we estimate that a cumulative ∼96.3 $GtCO_2$ of emissions are embedded in

deploying renewables and major adaptation-related interventions comprising the broader climate transition through 2100. These embedded emissions are strongly dominated by renewable deployment (i.e., fossil fuel combustion to power renewable energy deployment, ~95 $GtCO_2$), with a much smaller contribution from adaptive cooling and coastal protection and retreat (~1.3 $GtCO_2$, Fig. 3). Our estimates are by design conservative since they exclude non-CO_2 GHGs and other potential adaptation interventions such as inland flood protection (27) and water transfer infrastructure (28). More comprehensive estimates of energy demand from adaptation more generally across the economy will likely revise our estimates upwards (29). Further, other infrastructure required for decarbonization not considered in this study, such as new and modified electricity transmission networks, hydrogen production and storage facilities, and battery energy storage, will likely add considerable energy demands and embedded emissions (30–32). Despite this, our estimated magnitude of the emissions embedded in the transition is relevant to climate science and policy from several angles.

First, the emissions embedded in the transition are equivalent to a substantial mitigation effort. For instance, emissions under gradual decarbonization are 2.5 times (or 5 times for delayed decarbonization) larger than the total global emissions reductions attributable to national CO_2 abatement legislation over 1999 to 2016 (33). Further, they are on the order of (or for delayed decarbonization, about double) the emissions abatement from the United States hypothetically achieving net zero CO_2 emissions by 2050 (i.e., reducing emissions from ~5 to 0 $GtCO_2$/y over 30 y would avoid 75 $GtCO_2$/y, compared to constant emissions) (34). Relative to these measures, the emissions embedded in the transition are equivalent to a considerable climate legislative and mitigation effort. The emergence of these emissions in coming decades, which we argue is not explicitly researched or included in policy debates, has the potential to further complicate the challenge of meeting both adaptation and mitigation targets.

Second, total embedded emissions represent 5.5 to 8.6% of the remaining carbon budget within the respective scenarios. Furthermore, total transition emissions amount to 46% of the remaining carbon budget for 1.5 °C under delayed decarbonization (Fig. 5), which is the pathway most in line with current global policies. We argue that this latter mixed comparison is not contradictory, but rather accurately reflects the current global gap between climate commitments and actions. While international agreements affirm maximum warming targets of well below 2 °C and ideally 1.5 °C, national policies are in aggregate more consistent with the ~2.7 °C delayed transition scenario (21, 25). This comparison highlights an additional contradiction between global climate commitments and current actual policies

Since carbons budgets are commonly interpreted as the emissions runway after which global emissions must reach net zero (13), our results imply that a portion of this budget may need to be set aside for emissions embedded in the broader climate transition itself, effectively shortening the runway for other economic sectors. However, this qualitative conclusion of our analysis depends on whether these emissions should be regarded as outside (i.e., additional to) existing accounting of present and likely future emissions.

We note a few considerations on this question of additionality. First, some energy investment into renewable capacity will replace fossil fuel infrastructure at its planned retirement, representing capacity maintenance without net new energy demand. However, some degree of early retirement of fossil fuel infrastructure will be necessary to achieve more ambitious pathways (19, 35). From this perspective, the additionality of emissions embedded in the broader climate transition would be larger for faster-paced transitions necessitating more abandonment of fossil fueled capacity and premature replacement by renewables. Second, as with historical infrastructure investments, the interventions that we examine may stimulate household consumption and economic growth in other sectors. Prior to radical decarbonization of energy or decoupling of economic growth from energy, this would augment emissions (26, 36–38). However, the economic activity spurred by the transition could also divert economic growth from sectors that shrink during the transition. In short, these questions of additionality merit further research, being important to interpreting the relevance of embedded transition emissions for climate science and policy.

We find that emissions embedded in the broader climate transition are highly sensitive to transition pace (Fig. 4). This sensitivity arises mainly because the rate of renewable energy reinvestment into more renewables is limited importantly by slower deployment pace under a delayed transition (*SI Appendix*, Fig. S2*B*), strongly increasing fossil fuel use to deploy renewables (Fig. 4*B*) and thus embedded emissions (Fig. 4*C*), effectively creating an "emissions trap" (18). A consequence of this strong sensitivity is that lower climate ambition comes at a higher embedded emissions cost. However, we note that important questions exist surrounding the techno-political feasibility of the rapid decarbonization pathway and its associated large reduction in embedded transition emissions (26).

We show that deploying renewables will likely comprise the vast bulk of embedded emissions under the three pathways. Crucially, this implies that the majority of these emissions are intrinsic to the broader climate transition and likely unavoidable, as a certain amount of fossil fuel energy must be used to power initial renewable deployment. Until energy decarbonization has matured sufficiently, the fraction of energy embedded in deploying renewables that can be satisfied by renewables will be limited by low initial renewable capacity (*SI Appendix*, Fig. S2*A*). Thus, while emissions embedded in deploying renewables can be greatly reduced through ambitious decarbonization (Fig. 4*C*), they remain positive under all scenarios in our analysis. Nevertheless, avenues to minimize the energy and emissions intensity of deploying renewables exist, including employing renewable technologies with optimal energy return on energy invested (39) and alternatives to high-emissions materials like concrete and steel in construction, such as engineered wood (40).

As a broad global estimate spanning many complex sectors, our study has five important limitations that may be improved upon in future research. These limitations primarily influence our estimates of embedded emissions, and thus our quantitative conclusions. First, although our research provides insight and groundwork, it should be expanded to account for non-CO_2 emissions (notably N_2O, CH_4, and hydrofluorocarbons) and other emissions sources from mitigation and adaptation. Second, future model improvements may integrate dynamic interactions between interventions, such as energy system changes due to SLR impacts on coastal energy infrastructure, which may help elucidate other synergies or trade-offs between mitigation and adaptation. Third, in the absence of a solid observational basis, we make assumptions about the timing of coastal adaptations, whose influence on transition emissions should be further explored. Fourth, although we examine the sensitivity of our results to decarbonization pace and energy system assumptions, we otherwise rely on median socioeconomic and geophysical projections,

which in reality contain large uncertainties. Specifically, the sensitivity of transition emissions to high- or low-end projections of climate warming, SLR, global per-capita power requirements, and population and gross domestic product (GDP) growth should be explored further. Fifth, some equity concerns raised by our study should be further examined to ensure a just transition, including the dearth of coastal adaptation in sub-Saharan Africa in our results (*SI Appendix*, Fig. S1*A*), and the potential for mitigation emissions to be concentrated in wealthy, high-energy-use economies (41, 42).

A final limitation of our analysis is important to interpreting our qualitative conclusions: Because NETSET does not simulate economic considerations, they are omitted from our assessment of emissions embedded in deploying renewables. These factors merit future attention, notably around the function of capital markets, assumptions of energy decoupling from GDP growth, and their influences on the evolution of decarbonization and adaptation. Further, limiting emissions from deploying renewables may increase deployment costs, a factor crucial to translating our results into appropriate policy action. Depending on the magnitude of these costs, abating emissions from deploying renewables may be more costly than offsetting them elsewhere in the economy. Our results provide an initial quantitative basis for calibrating these decisions, suggesting that emissions embedded in deploying renewables should be considered in modeling cost-optimal transition pathways.

Despite these limitations, we conclude that the magnitude of CO_2 emissions embedded in the broader climate transition are of geophysical and policy relevance. In addition, transition emissions can be greatly reduced under faster-paced decarbonization, lending new urgency to policy progress on rapid renewable energy deployment. Most fundamentally, our results point to underappreciated synergies and trade-offs between mitigation goals and emissions embedded in deploying renewables, which must be better understood and integrated into climate policy for an effective transition.

Materials and Methods

Overall Framework and Scope. To estimate the probable embedded emissions from mitigation and adaptation through the broader climate transition, we must first establish a limited scope of sectoral interventions. It is impossible to exhaustively account for the diverse changes required to mitigate and adapt to climate change globally, which involve a vast array of changes at household, institutional, national, and international scales. We instead focus on interventions that satisfy three criteria, which we treat as proxies for the global gross energetic and material magnitude of the interventions, as well as the likelihood of them being implemented.

First, we constrain our scope to interventions responding to global-scale changes (e.g., adaptation to SLR, deployment of solar and wind power) rather than ones that are limited to specific environments (e.g., adaptation to or reducing emissions from melting permafrost). Second, we focus on plausibly energy- and material-intensive options for adaptation (for instance, constructing new coastal protections as opposed to breeding heat-tolerant crop varieties) and mitigation (for instance, building wind turbines as opposed to reducing deforestation). Finally, we focus on adaptation to aspects of climate change projected with high confidence (e.g., sea levels and mean temperatures are very likely to rise and not fall), rather than aspects with greater directional uncertainty and higher regional and temporal variability (e.g., hydrological drought may increase or decrease in many places). We assert that high confidence in the direction of such changes translates to high confidence in the eventuality of the interventions.

Following these criteria, three sectoral interventions are likely to be among the largest sources of emissions, enabling a simple but conservative estimate of the rough magnitude. These are 1) deploying renewables, or the construction of renewable electricity generating capacity and associated infrastructure; 2) coastal adaptation, including protection and retreat; and 3) adaptive enhancement of space cooling. This list is a small sample of the likely total mitigation and adaptation effort, and in this sense our estimated emissions from mitigation and adaptation are by design a lower bound. Furthermore, many of the key economic, energy, and policy interactions among mitigation and adaptation interventions remain frontiers of research with dramatic uncertainties (5, 7, 43, 44). We therefore conceptually simplify our analysis by neglecting some potential interactions among these interventions, instead treating them as independent (e.g., we neglect future coastal retreat as a potential barrier or boon to deployment of offshore wind). We further limit our focus to CO_2 as the main anthropogenic GHG.

For each of the three interventions (subscripts i), we conceptualize embedded emissions ($E_{i,t}$) as the amount of each activity ($N_{i,t}$) times its emissions intensity ($I_{i,t}$), both of which evolve over the years of the transition (subscript t). The cumulative total embedded emissions from mitigation and adaptation (E_{M+A}) interventions through the transition is the sum over i and t:

$$E_{M+A} = \sum_{i,t} E_{i,t} = \sum_{i,t} N_{i,t} I_{i,t}. \quad [1]$$

This simple governing equation decomposes the task of emissions estimation into two components: modeling adaptation and mitigation activities over time, and estimating their emissions intensities. Data limitations constrain the spatial scale of the equation to the global aggregate, precluding the examination of differences between countries' mitigation and adaptation pathways and emissions intensities. The time dependence of the terms in Eq. **1** relates to the pace of energy decarbonization, as well as population and economic trends. We use a broadly consistent set of input GDP and population projections from the UN median scenario (45), shared socioeconomic pathways (SSPs) (46), and other sources (6, 10, 12). We examine the transition over the period 2020 to 2100.

The amount of each intervention over time is estimated using a suite of sectoral models, namely, the NETSET model V2.0 (12), the CIAM V1 (6), and the EDGE (10). To estimate emissions intensities of the interventions over time, we generally first estimate the energy intensity of the intervention based on the literature and then convert the energy to emissions depending on the energy mix evolution from the NETSET runs and the emissions intensities of fossil fuels from the literature. For the case of coastal retreat and protection, we separately assess process emissions arising from chemical reactions in material production (i.e., CO_2 released by chemical reactions in concrete and steel production). The methods for the sectoral modeling and emissions accounting are discussed in the following sections. The complete methods are summarized in *SI Appendix*, Fig. S5.

Decarbonization Pathways. We use the NETSET energy transition model to simulate the replacement of fossil fuels with renewables and the investment of energy into bringing the renewable capacity online (i.e., the energy embedded in deploying renewables) through 2100. As a net energy model, NETSET is suited to this task, explicitly simulating energy investments into energy via variation in energy return on energy invested (EROEI) across primary energy sources. Meanwhile, the main limitation of NETSET is incomplete representation of economic dynamics (e.g., capital markets, technological diffusion, and economy-energy feedbacks beyond EROEI dynamics). The model functions as a globally aggregated back-casting model that simulates plausible transition pathways satisfying the preconditions that 1) geophysical carbon budgets for assumed warming targets are not exceeded (see section Emissions Accounting below), and 2) a minimum net primary power per person of 2,000 W is met by the global energy system (net meaning excluding energy investment into energy). Other important model dynamics included assumed fossil fuel phase-out start date; scale limitations for hydroelectricity, nuclear, geothermal, and biomass; as well as assumptions about future learning rates in deployment of solar and wind. The energetic contribution of fossil fuels through the transition is determined based on Hubbert curves with assumed peak extraction in 2020. We use a uniform peak extraction year across scenarios to isolate the influence of transition pace, rather than time of onset. Finally, the deployment of scalable renewables (i.e., solar photovoltaic, compact solar power, geothermal, and wind) dynamically responds to the time evolution of fossil fuels and scale-limited renewable capacity, subject to the per-capita energetic and carbon budget preconditions. Energy investment into renewables is allocated across energy sources based on the gross energy mix and EROEI of different energy sources, and

we track the fraction of renewable energy reinvestment as a key determinant of embedded emissions. NETSET is open-source (https://set.csaladen.es/) and further model details can be found in ref. 12. We focus first on a gradual decarbonization pathway assuming a carbon budget of 1,150 $GtCO_2$ from 2020 onwards, corresponding to a warming cap of 2 °C assuming a 67th percentile transient climate response to cumulative emissions (TCRE) (21). This scenario is broadly consistent with the Intergovernmental Panel on Climate Change RCP 2.6 emissions scenario in terms of cumulative total emissions and ensuing climate-model projected warming (47). Note that because NETSET does not include negative emissions, the simulations do not allow temporary overshoot of the warming targets, and thus project somewhat faster decarbonization than scenarios allowing negative emissions (4). We then examine the sensitivity of embedded transition emissions to delayed and rapid decarbonization pathways. For the delayed case, we stipulate a carbon budget of 2,150 $GtCO_2$, linked to a warming of 2.7 °C in 2100 (67th percentile TCRE) and broadly consistent with RCP 4.5 emissions scenario in terms of cumulative total emissions and warming. This scenario is in line with the current global aggregate of actual climate policies, and thus reflects a likely pathway in the absence of strong climate policy ambition. For the rapid case, we stipulate a carbon budget of 400 $GtCO_2$ linked to a warming cap of 1.5 °C, consistent the 2015 Paris Agreement. Together, these scenarios reflect the plausible range of decarbonization pace, including highly ambitious (rapid), moderately ambitious (gradual), and "current policies" (delayed) pathways.

We test the sensitivity of estimated embedded emissions from deploying renewables to two key energy system assumptions in NETSET: future net primary power per person and the fossil fuel phase-out start date. We assess fossil fuel phase-out years including 2020 (our default assumption), 2030, and 2040, combined with per capita power demand of 2,000 W (our default assumption), 2,500 W, and 3,000 W. In total, this yields eight sensitivity cases beyond the default assumptions. Emissions from deploying renewables vary by 5% on average across parameter pairs compared to default assumptions, with maximum emissions increase under the high power, late phase-out pair, where emissions increase by 21% (*SI Appendix*, Fig. S3). These variations are generally an order of magnitude smaller than those across decarbonization pathways, suggesting relatively low dependence of embedded emissions from deploying renewables on NETSET model parameters.

We simulate these three decarbonization pathways using NETSET (12) and use these simulations as the energy system backbone for the remaining modeling in this study. First, the simulations enable the estimation of emissions embedded in the transition by providing time series of coal, oil, and natural gas energy investment into renewables (N_{SET}). Second, they enable the estimation of the emissions intensity of global energy use for the three adaptation interventions via time series of energy mix.

Adaptive Space Cooling. To estimate future adaptive energy demand for space cooling, we use the EDGE building energy modeling framework (10). EDGE expands the SSPs (46, 48, 49) to project consistent changes in building floor space demand (positively related to GDP and total population, negatively to population density) and building envelope and appliance efficiencies (both assumed to increase with technological improvement). In EDGE, per capita cooling energy demand responds to climate warming in two ways. As hot days increase with climate warming, a larger proportion of the global population acquires cooling equipment, and each cooling appliance is used more intensively. Simulated cooling demand is also influenced by population growth, efficiency improvements in cooling appliances and building envelopes, and income per capita, which augments floor space per capita and the relative affordability of air conditioning. Additional details on the EDGE framework can be found in ref. 10.

Future CDDs are projected based on Coupled Model Intercomparison Project Phase 5 (CMIP5) climate model runs under the RCP emissions scenarios. In this setup, CDDs are computed as the sum of daily degrees above an assumed thermostat set point temperature of 21 °C. Gridded temperature projections from the climate models are weighted by population density in their aggregation to the national scale. In this study, we use final energy demand projections from EDGE run under the "middle-of-the-road" SSP2 and with CDD projections from RCP2.6 for gradual decarbonization and RCP4.5 for the delayed scenario. For the rapid pathway, we rescale the RCP2.6 CDD projections based on the global difference in mean warming between the 2.0 °C and 1.5 °C pathways, as explicit CDD projections for this scenario are under development.

Population, income, and insulation dynamics are assumed to be the same for all decarbonization pathways to isolate the impact of climate change from socioeconomic trends. We further isolate the climate-adaptive component of projected energy demand for each pathway by subtracting energy demand projections under a constant historical climatology from the runs with warming. This assumes that expanding cooling due to socioeconomic trends (e.g., first-time acquisition of air conditioners newly enabled by rising incomes) is not itself climate adaptive. We convert final to primary energy demand for cooling by first estimating the global primary-to-final energy conversion efficiency based on global mean power station conversion efficiencies from the Interational Energy Agency (IEA), averaged over the 5 most recent years with available data (2014 to 2018) (50). We update this primary-to-final ratio through the decarbonization pathway based on the energy mix evolution in NETSET, assuming a primary-to-final energy ratio of 1 for renewables. We finally report climate-adaptive space cooling as primary energy demand, which we treat as the relevant input to the emissions accounting.

In contrast to space cooling, which is largely powered by electricity, space heating is fueled by a diversity of carriers. Because NETSET does not explicitly simulate energy demand, carriers, and conversion methods for space heating, major offline energy-system assumptions are required to estimate future emissions reductions from this substantial global energy use. This limitation results in large uncertainties for these results for heating, so we caveat them by omitting them from main figures. Conforming to the fossil fuel phase-out simulated in each decarbonization pathway, we assume a transition from fossil fuel combustion heating to a heating energy regime in which final heating energy demand is evenly split across six carriers: electric resistance heating, electric heat pumps, traditional biofuels, modern biofuels, district electric heat pumps, and district biofuel heating. Similar to space cooling, final energy demand is simulated in EDGE based on the above scenario based on projected changes in heating degree days under the respective climate model simulations. To estimate primary energy demand, we assume 1:4 primary-to-final efficiency of all heat pumps and conversion efficiencies of 0.7 for traditional biofuels, 0.8 for modern biofuels, 0.95 for oil and gas furnaces, and 0.85 for coal furnaces. As for space cooling, we isolate the climate-adaptive component of energy and emissions by differencing the runs with climate change from counterfactual runs with constant historical climatology.

Coastal Adaptation: Retreat and Protection. CIAM is a global cost-optimization model that assesses coastal impacts and least-cost-optimal adaptation decisions for ∼12,000 individual coastline segments (6). The biophysical and socioeconomic data for the segments originate from the dynamic interactive vulnerability assessment dataset (DIVA, in turn based on 30 arcsec digital elevation model) (51). The model code is open source and publicly available from https://github.com/delavane/CIAM. The decision set includes construction of coastal protection (conceived of here as a sea dike), coastal retreat (conceived of reconstruction of coastal settlements further inland), or no adaptation (with associated flood damage and loss of coastal land). The model assimilates diverse socioeconomic and geophysical data, notably from the DIVA coastline dataset (51), to estimate protection, retreat, and flood damage costs as well as the value of inundated coastal land (land value) and wetlands (value of wetland ecosystem services). For each segment, the optimal decision is that which minimizes the sum of these costs under projected SLR for an assumed planning period. Beyond the optimal decision category, the model also provides optimal quantities for retreat (the retreat perimeter defined as an elevation above sea level, from which retreat population can be derived) and protection (the optimal dike height).

CIAM's main strength is its integration of top-down geophysical drivers of risk with bottom-up socioeconomic variables (e.g., GDP, land value, and population, broadly consistent with SSP2) that are essential to understanding probabilities of coastal protection and retreat. Its main limitation is that a relatively circumscribed set of socioeconomic variables are considered, excluding hard-to-quantify ones reflecting local political or cultural barriers to or enablers of retreat and protection (7, 43, 52). These factors could lead to outcomes that deviate from cost optimality. Further, cost "optimal" decisions under this framework are not necessarily equitable or socially preferred due to a dominant influence of GDP as a proxy of capital density on model adaptation decisions. As a result, CIAM projects that large parts of the Global South with high population but low capital density will remain unprotected through 2100.

Our CIAM implementation stipulates an adaptation planning horizon of 2050 to 2100 in which decision making accounts for sea level in 2050 and projected SLR to 2100 (53) (i.e., we assume planners use a unified set of sea level projections). This planning horizon allows the three decarbonization pathways to have differential influences on adaptation decisions, as SLR projections do strongly depend on emissions scenarios prior to 2050. The optimization is run for 10-y time steps over this 50-y planning time horizons. In each time step, the historical flood statistics for each coastal segment are incremented by locally downscaled SLR projections, modifying the cost function and thus the optimal decision over time. We then aggregate the incremental adaptations over the planning horizon into a single projected adaptation decision responding to projected SLR for the period. Because CIAM does not simulate when within the 50-y planning horizon adaptations will be built, we assume that all coastal adaptations occur in 2060. This provides a reasonable 10 y after the start of the planning period for adaptations to roll out, and the time midpoint of the transition as defined by our analysis period.

Projected mean SLR is based on ref. 53 which downscales global SLR projections to the local scale. This dataset increments circa-2000 historical sea level distributions, estimated from global tide gauge data, by projected thermal expansion, land-based ice melt, land water storage, and other terms, driven by RCP2.6 for gradual decarbonization and RCP4.5 for the delayed case. High-resolution downscaled SLR projections are still under development for the 1.5 °C rapid pathway, so in the interim, we estimate them by decrementing those for RCP2.6 by the global mean difference in sea level rise between 2.0 °C and 1.5 °C (54).

A central method in CIAM for the present study involves accounting for extreme sea levels, which determine retreat perimeter and protection height via their influence on flood damage costs and subsequent optimization. The DIVA dataset reports estimated 1-in-1, -10, -100, and -1,000 y storm surge heights, which are used in CIAM along with SLR projections to estimate expected values of the flood damage in the cost optimization. Thus, cost-optimal retreat perimeters and protection heights are ultimately based on these underlying surge height levels. To account for initial adaptation in the absence of comprehensive global data on coastal protective infrastructure, CIAM's default assumption is that global coastlines are initially protected to the 1-in-1 y (i.e., mean annual maximum) storm surge height (S_1) at the beginning of the planning period. Here, we modify this assumption to better reflect widespread underprotection of global coastlines (55), asserting instead that all coastal segments are initially protected to one-half of the 1-in-1 y storm surge.

In the absence of LCA literature for coastal protection infrastructure, we developed a simple geometric model of a generic dike based on technical literature (56, 57) to estimate the volume of sea dike materials as a function of optimal protection height (H_{opt}) and coastal segment length (*SI Appendix*, Fig. S6). To convert the optimal protection height to sea dike build height, we increment the optimal protection height by the climatological maximum wave height from DIVA to incorporate a realistic wave run-up height (W_C) into the dike design. Thus, the full protection height including initial adaptation is given by:

$$H = H_{opt} + \frac{1}{2}S_1 + W_C. \quad [2]$$

We then model the dike as a trapezoid in cross-section with berm width b of 5 m, slopes m_1 and m_2 of 1:4 on the seaward side and 1:3 on the landward side, and a reinforced concrete foundation with thickness of $F = 1/4H$. We assume the dike to be filled with local soil and rock (and thus neglect transport emissions) and encased in a revetement of medium-strength steel reinforced concrete with thickness T equal to 1 m. We treat the sum over coastal segments s of the volume of reinforced concrete in the dikes (N_{CP}), which is quadratic in build height, as the main driver of coastal protection emissions. This volume is the product of the cross-sectional area of the concrete revetement and the coastline segment length (L_s):

$$N_{CP} = \sum_s L_s \left\{ \frac{1}{4}(m_1 + m_2 + b)H^2 + (m_1 + m_2)HT - \frac{1}{2}(m_1 + m_2)T^2 + (m_1 + m_2)T \right\}. \quad [3]$$

For the case of coastal retreat, we treat the number of households retreated (N_{CR}) as the driver of emissions, assuming an equivalent number of new dwellings will be constructed to accommodate them. Retreat population is estimated by first converting the retreat perimeter height to retreat area using elevation-area functions in DIVA and then multiplying the retreat area by population density (also from DIVA). Due to a lack of supporting literature, we neglect emissions likely to result from energy embedded in the removal of abandoned housing and infrastructure.

Emissions Accounting. The sectoral modeling approaches enable an estimation of the adaptation amount ($N_{i,t}$) terms in Eq. **1**. The remaining ingredient is to estimate the emissions intensities of the interventions ($I_{i,t}$), which we accomplish by combining with LCA literature and databases with NETSET energy mix projections (*SI Appendix*, Table S1). First, we estimate the global mean emissions intensity of primary energy (I_F) for the three fossil fuel classes in NETSET (coal, oil, and gas) which are then used to compute emissions from space cooling and coastal adaptation energy demand. The emissions intensity of energy use from coal, oil, and natural gas is estimated as the 2018 to 2050 average of projected global energy–related emissions by fuel class divided by the total energy use by fuel class based on data from the US Energy Information Administration International (EIA) Energy Outlook 2019 (*SI Appendix*, Table S1). Note that this approach does not assimilate EIA energy mix projections, but only emissions intensity projections. We neglect emissions from the extraction and processing of nuclear fuels and assume zero emissions from other nonfossil fuel energy carriers such as fugitive emissions from geothermal- and hydroelectric- and nonenergy-related build emissions for solar and wind (e.g., process emissions from steel).

To estimate the cumulative emissions embedded in deploying renewables, we first estimate the global emissions intensity of overall primary energy use over time ($I_{E,t}$ in units of mass of CO_2 per unit primary energy use) by weighting the emissions intensities per fuel f by their share in the energy mix as projected in NETSET($x_{f,t}$). We then simply multiply projected energy investment into energy (N_{SET}) by $I_{E,t}$, the global emissions intensity of energy, and sum across the transition period:

$$E_{SET} = \sum_t N_{SET,t} I_{E,t} = \sum_t N_{SET,t} \sum_f x_{f,t} I_f. \quad [4]$$

We follow a similar equation to convert adaptive cooling energy demand to emissions. While space cooling is linked to certain potent nonenergy GHG emissions such as hydrofluorocarbons, we limit the scope of our assessment to CO_2.

For construction of sea dikes, we use emissions factors and embedded energy estimates for construction materials from ref. 58. Assuming a density of concrete of 2,400 kg/m^3 and 150 kg of reinforcing steel per m^3 (59, 60), we calculate a volumetric emissions factor to convert global total volume of sea dike revetement (N_{CP}, Eq. **3**) to emissions. We neglect emissions from rock and soil transport for the dike interior as well as from site preparation. For coastal retreat, we assume resettlement will be directed toward medium density urban developments and base our emissions factor on recent LCA estimates of CO_2 emissions and embedded energy (E) arising from these constructions per unit of floor area (61, 62). These estimates include some necessary infrastructure beyond dwellings themselves, such as roads, but are not comprehensive (e.g., they do not include water systems). To convert between retreat population and retreat dwellings, we assume a mean household size of five people (Pew Research Center, 2019), and a dwelling ground area of 225 m^2 as in EDGE (10).

For dikes and resettlement, the emissions intensity incorporates both fossil fuel energy use and nonenergy process emissions from materials such as cement and steel production. To account for decarbonization of energy in the future, we update the emissions factors for dikes and resettlement at time t by rescaling emissions due to embedded energy (E) by the difference in emissions intensity of energy (I_E) between time t and prior to the transition (t_0):

$$I_{i,t} = I_{i,t_0} + E(I_{E,t} - I_{E,t_0}). \quad [5]$$

We further rescale the nonenergy process emissions from cement and steel for coastal protection to account for future mitigation from technological improvements in these industries. To do so, we decrease the current process emissions intensity of steel and cement over time based on the fractional reduction in emissions intensities under the sustainable development scenarios in the International Energy Agency's Technology Roadmaps for iron and steel (23) and cement (24). These scenarios only include emissions reduction estimates for 2030 and 2050, so we interpolate them to 10-y time steps between 2020 and 2060, and, in the absence of any basis for further mitigation, assume stationary emissions intensities beyond 2060. The precision of the timing of adaptation decisions from CIAM is limited to 50-y planning horizons, so we simply assume that all coastal retreat and protection occurs at the midpoint of the transition in

2060. We neglect emissions from the operation and maintenance of relocated housing and coastal protection.

The final aspect of emissions accounting is to contextualize the emissions embedded in the transition relative to relevant benchmarks. To understand the magnitude of emissions on an Earth system scale, we express transition emissions as a fraction of the remaining carbon budget for the respective pathways (1,150 $GtCO_2$ for gradual, 2,150 $GtCO_2$ for delayed, and 400 $GtCO_2$ for rapid) (21).

Data, Materials, and Software Availability. The data underlying this study are publicly available from the sources indicated in *SI Appendix*, Table S1. All intermediate data and analysis code are available from https://www.github.com/clesk/transition-embedded-emissions, (63). Underlying model code and input data are open source and publicly available from the URLs in *Materials and Methods*. Code for the EDGE model is available from R.H. upon request.

ACKNOWLEDGMENTS. We thank Anton Safonov, Delavane Diaz, Ethan Coffel, David Chen, Justin Mankin, and Caleb Gingrich Regehr for helpful discussions of methods and results. We acknowledge the World Climate Research Programme, which, through its Working Group on Coupled Modelling, coordinated CMIP5, and we thank the climate modeling groups for producing and making available their model output. This material is based upon work supported by the National Science Foundation Graduate Research Fellowship under Grant DGE 1644869. The research from R.H. and A.L. was funded by the German Federal Ministry of Education and Research under Grant 03SFK5A (Copernicus Project Ariadne).

Author affiliations: [a]Ocean and Climate Phyiscs, Lamont-Doherty Earth Observatory, Palisades, NY, 10964; [b]Earth and Environmental Science, Columbia University, New York, NY, 10027; [c]School of Engineering, Lancaster University, Lancaster, LA1 4YW, United Kingdom; [d]Economics Observatory, School of Economics, University of Bristol, Bristol, BS8 1TH, United Kingdom; [e]Faculty of Economics and Business Administration, Babes-Bolyai University, Cluj-Napoca, 400084, Romania; [f]Potsdam Institute for Climate Impact Research, Member of the Leibniz Association, Potsdam, 14473, Germany; [g]Research and Development Center, Dubai Electricity and Water Authority, Dubai, UAE; [h]Department of Environmental Science and Policy, Rosenstiel School of Marine and Atmospheric Science, University of Miami, Miami, FL, 33149; [i]Leonard and Jayne Abess Center for Ecosystem Science and Policy, University of Miami, Coral Gables, FL, 33124; and [j]Department of Geography, Planning, and Environment, Concordia University, Montréal, QC, H3G 2E9, Canada

1. S. I. Seneviratne, M. G. Donat, A. J. Pitman, R. Knutti, R. L. Wilby, Allowable CO2 emissions based on regional and impact-related climate targets. *Nature* **529**, 477–483 (2016).
2. C. F. Schleussner *et al.*, Science and policy characteristics of the Paris Agreement temperature goal. *Nat. Clim. Chang.* **6**, 827–835 (2016).
3. R. Knutti, J. Rogelj, J. Sedlácek, E. M. Fischer, A scientific critique of the two-degree climate change target. *Nat. Geosci.* **9**, 13–18 (2016).
4. J. Rogelj *et al.*, Scenarios towards limiting global mean temperature increase below 1.5°C. *Nat. Clim. Chang.* **8**, 325–332 (2018).
5. V. Viguié *et al.*, When adaptation increases energy demand: A systematic map of the literature. *Environ. Res. Lett.* **16**, 033004 (2021).
6. D. B. Diaz, Estimating global damages from sea level rise with the Coastal Impact and Adaptation Model (CIAM). *Clim. Change* **137**, 143–156 (2016).
7. M. E. Hauer *et al.*, Sea-level rise and human migration. *Nat. Rev. Earth Environ.* **1**, 28–39 (2020).
8. D. Lincke, J. Hinkel, Coastal migration due to 21st century sea-level rise. *Earths Futur.* **9**, 1–14 (2021).
9. A. R. Siders, M. Hino, K. J. Mach, The case for strategic and managed climate retreat. *Science* **365**, 761–763 (2019).
10. A. Levesque *et al.*, How much energy will buildings consume in 2100? A global perspective within a scenario framework. *Energy* **148**, 514–527 (2018).
11. J. Hinkel *et al.*, Coastal flood damage and adaptation costs under 21st century sea-level rise. *Proc. Natl. Acad. Sci. U.S.A.* **111**, 3292–3297 (2014).
12. S. Sgouridis, D. Csala, U. Bardi, The sower's way: Quantifying the narrowing net-energy pathways to a global energy transition. *Environ. Res. Lett.* **11**, 094009 (2016).
13. H. D. Matthews *et al.*, Opportunities and challenges in using remaining carbon budgets to guide climate policy. *Nat. Geosci.* **13**, 769–779 (2020).
14. M. Z. Jacobson *et al.*, 100% clean and renewable wind, water, and sunlight all-sector energy roadmaps for 139 countries of the world. *Joule* **1**, 108–121 (2017).
15. J. Rogelj, D. L. McCollum, A. Reisinger, M. Meinshausen, K. Riahi, Probabilistic cost estimates for climate change mitigation. *Nature* **493**, 79–83 (2013).
16. N. P. Myhrvold, K. Caldeira, Greenhouse gases, climate change and the transition from coal to low-carbon electricity. *Environ. Res. Lett.* **7**, 014019 (2012).
17. K. C. Seto *et al.*, Carbon lock-in: Types, causes, and policy implications. *Annu. Rev. Environ. Resour.* **41**, 425–452 (2016).
18. M. R. Sers, P. A. Victor, The energy-missions trap. *Ecol. Econ.* **151**, 10–21 (2018).
19. D. Tong *et al.*, Committed emissions from existing energy infrastructure jeopardize 1.5 °C climate target. *Nature* **572**, 373–377 (2019).
20. G. Luderer *et al.*, Residual fossil CO2 emissions in 1.5-2°C pathways. *Nat. Clim. Chang.* **8**, 626–633 (2018).
21. J. G. Canadell *et al.*, "Global carbon and other biogeochemical cycles and feedbacks" in *Climate Change 2021: The Physical Science Basis. Contribution of Working Group I to the Sixth Assessment Report of the Intergovernmental Panel on Climate Change*, V. Masson-Delmotte *et al.*, Eds. (Cambridge University Press, 2021), **vol. P**.
22. M. Lenzen, J. Munksgaard, Energy and CO2 life-cycle analyses of wind turbines-review and applications. *Renew. Energy* **26**, 339–362 (2002).
23. International Energy Agency, "Iron and Steel Technology Roadmap: Towards more sustainable steelmaking." (Paris, France, 2020).
24. International Energy Agency, "Technology Roadmap - Low-Carbon Transition in the Cement Industry." (Paris, France, 2018).
25. UNEP. *Emissions Gap Report* **2020**, 1–102 (2020).
26. L. T. Keyßer, M. Lenzen, 1.5 °C degrowth scenarios suggest the need for new mitigation pathways. *Nat. Commun.* **12**, 2676 (2021).
27. F. Dottori *et al.*, Increased human and economic losses from river flooding with anthropogenic warming. *Nat. Clim. Chang.* **8**, 781–786 (2018).
28. Y. Qin *et al.*, Agricultural risks from changing snowmelt. *Nat. Clim. Chang.* **10**, 459–465 (2020).
29. F. P. Colelli, J. Emmerling, G. Marangoni, M. N. Mistry, E. De Cian, Increased energy use for adaptation significantly impacts mitigation pathways. *Nat. Commun.* **13**, 4964 (2022).
30. M. Zeyringer, J. Price, B. Fais, P. H. Li, E. Sharp, Designing low-carbon power systems for Great Britain in 2050 that are robust to the spatiotemporal and inter-annual variability of weather. *Nat. Energy* **3**, 395–403 (2018).
31. A. E. MacDonald *et al.*, Future cost-competitive electricity systems and their impact on US CO2 emissions. *Nat. Clim. Chang.* **6**, 526–531 (2016).
32. S. Sgouridis, M. Carbajales-Dale, D. Csala, M. Chiesa, U. Bardi, Comparative net energy analysis of renewable electricity and carbon capture and storage. *Nat. Energy* **4**, 456–465 (2019).
33. S. M. S. U. Eskander, S. Fankhauser, Reduction in greenhouse gas emissions from national climate legislation. *Nat. Clim. Chang.* **10**, 750–756 (2020).
34. US Environmental Protection Agency, "Inventory of U.S. greenhouse gas emissions and sinks: 1990-2019" (2021).
35. A. Pfeiffer, C. Hepburn, A. Vogt-schilb, B. Caldecott, Committed emissions from existing and planned power plants and asset stranding required to meet the Paris Agreement, *Envrion. Res. Lett.* **13**, 054019 (2018).
36. S. Fankhauser, R. S. J. Tol, On climate change and economic growth. *Resour. Energy Econ.* **27**, 1–17 (2005).
37. A. Grubler *et al.*, A low energy demand scenario for meeting the 1.5°C target and sustainable development goals without negative emission technologies. *Nat. Energy* **3**, 515–527 (2018).
38. D. Horen Greenford, T. Crownshaw, C. Lesk, K. Stadler, H. D. Matthews, Shifting economic activity to services has limited potential to reduce global environmental impacts due to the household consumption of labour. *Environ. Res. Lett.* **15**, 064019 (2020).
39. K. P. Bhandari, J. M. Collier, R. J. Ellingson, D. S. Apul, Energy payback time (EPBT) and energy return on energy invested (EROI) of solar photovoltaic systems: A systematic review and meta-analysis. *Renew. Sustain. Energy Rev.* **47**, 133–141 (2015).
40. M. H. Ramage *et al.*, The wood from the trees: The use of timber in construction. *Renew. Sustain. Energy Rev.* **68**, 333–359 (2017).
41. K. Hubacek *et al.*, Global carbon inequality. *Energy Ecol. Environ.* **2**, 361–369 (2017).
42. H. D. Matthews, Quantifying historical carbon and climate debts among nations. *Nat. Clim. Chang.* **6**, 60–64 (2016).
43. R. M. Horton, A. de Sherbinin, D. Wrathall, M. Oppenheimer, Assessing human habitability and migration. *Science* **372**, 1279–1283 (2021).
44. A. Lesnikowski *et al.*, What does the Paris Agreement mean for adaptation? *Clim. Policy* **17**, 825–831 (2017).
45. United Nations Department of Economic and Social Affairs, Population Division. "World Population Prospects 2019: Data Booket" (2019).
46. S. Kc, W. Lutz, The human core of the shared socioeconomic pathways: Population scenarios by age, sex and level of education for all countries to 2100. *Glob. Environ. Change* **42**, 181–192 (2017).
47. M. Meinshausen *et al.*, The RCP greenhouse gas concentrations and their extensions from 1765 to 2300. *Clim. Change* **109**, 213–241 (2011).
48. B. C. O'Neill *et al.*, The roads ahead: Narratives for shared socioeconomic pathways describing world futures in the 21st century. *Glob. Environ. Change* **42**, 169–180 (2017).
49. R. Dellink, J. Chateau, E. Lanzi, B. Magné, Long-term economic growth projections in the Shared Socioeconomic Pathways. *Glob. Environ. Change* **42**, 200–214 (2017).
50. IEA, "World Energy Balances: Overview." (Paris, France, 2021).
51. A. T. Vafeidis *et al.*, A new global coastal database for impact and vulnerability analysis to sea-level rise. *J. Coast. Res.* **24**, 917–924 (2008).
52. K. J. Mach, A. R. Siders, Reframing strategic, managed retreat for transformative climate adaptation. *Science* **372**, 1294–1299 (2021).
53. R. E. Kopp *et al.*, Probabilistic 21st and 22nd century sea-level projections at a global network of tide-gauge sites. *Earths Futur.* **2**, 383–406 (2014).
54. Department of Dike Management & Flood Control. *Technical Guidelines on Sea Dike Design*. Vietnam Ministry of Agriculture and Rural Development. (Hanoi, Vietnam, 2011).
55. B. Fox-Kemper *et al.*, Ocean, cryosphere and sea level change. Clim. Chang. 2021 Phys. Sci. Basis. Contrib. Work. Gr. I to Sixth Assess. Rep. Intergov. Panel Clim. Chang. Basis. Contrib. Work. Gr. I to Sixth Assess. Rep. Intergover. **2018**, 1–257 (2021).
56. C. McMichael, S. Dasgupta, S. Ayeb-Karlsson, I. Kelman, A review of estimating population exposure to sea-level rise and the relevance for migration. *Environ. Res. Lett.* **15**, 123005 (2020).
57. S. N. Jonkman, M. M. Hillen, R. J. Nicholls, W. Kanning, M. Van Ledden, Costs of adapting coastal defences to sea-level rise - New estimates and their implications. *J. Coast. Res.* **29**, 1212–1226 (2013).
58. Pew Research Center, "Religion and Living Arrangements Around the World" (2019).
59. G. P. Hammond, C. I. Jones, Embodied energy and carbon in construction materials. *Proc. Inst. Civ. Eng. Energy* **161**, 87–98 (2008).
60. D. Kellenberger *et al.*, Life Cycle inventories of Building Products. *Ecoinvent report No.7*, Swiss Center for Life Cycle Inventories, Dübendorf (2007).
61. J. Monahan, J. C. Powell, An embodied carbon and energy analysis of modern methods of construction in housing: A case study using a lifecycle assessment framework. *Energy Build.* **43**, 179–188 (2011).
62. N. C. Kayaçetin, A. M. Tanyer, Embodied carbon assessment of residential housing at urban scale. *Renew. Sustain. Energy Rev.* **117**, 109470 (2020).
63. C. Lesk *et al.*, transition-embedded-emissions. GitHub. https://github.com/clesk/transition-embedded-emissions. Deposited 13 October 2022.